

Thermal boundary resistance to solid helium, hydrogen, deuterium, and neon*

C. L. Reynolds, Jr. and A. C. Anderson

*Department of Physics and Materials Research Laboratory, University of Illinois at Urbana-Champaign,
Urbana, Illinois 61801*

(Received 29 April 1976)

Measurements have been made in the temperature range 1–3 K of the thermal boundary resistance R_B between copper and solid ^4He , H_2 , D_2 , and Ne. The data for solid Ne agree within $\approx 20\%$ with the acoustic mismatch theory. However, the magnitude of R_B to solid H_2 or D_2 is found to be anomalously small, as for liquid or solid He, which is consistent with the earlier, complementary measurements of phonon reflection coefficients by Buechner and Maris.

I. INTRODUCTION

An acoustic mismatch model has been developed¹⁻⁵ to explain the origin of the thermal boundary resistance that exists in the presence of non-electronic heat transport across the interface between dissimilar materials. This model, which is discussed in Sec. II, predicts the boundary resistance between a variety of solids with an accuracy of order 10% in the temperature range from 0.01 to 100 K using no adjustable parameters.^{4, 6, 7} Somewhat less quantitatively, the model also appears to be valid for the interface between liquid helium and carefully prepared copper,⁸ but only for temperatures $T \lesssim 0.1$ K. At higher temperatures the measured boundary resistance R_B is less than that calculated from the model. At 1–2 K the discrepancy is a factor of ≈ 100 .

Recent measurements⁹ indicate that the acoustic mismatch mechanism does contribute to the heat transfer from a solid to liquid helium near 1 K, but that a second, unknown mechanism dominates the process. The unknown mechanism is very frequency dependent,¹⁰ and it is this frequency dependence which is reflected in the rather abrupt change in R_B between 0.1 and 1 K. Transverse as well as longitudinal phonons incident on the interface from the solid contribute to the thermal exchange¹¹ in a process which is inelastic or nonlinear as evidenced by the frequency conversion of the phonons.¹² As helium is added to the interface a monolayer at a time, the unknown mechanism appears to be activated at roughly the second monolayer.¹²

The dominant heat-transfer mechanism has not been identified. One question that has been asked in an attempt to limit the possible choice is whether the anomaly occurs for materials other than liquid ^4He . It has been demonstrated that R_B near 1 K is essentially the same for liquid or solid ^3He or ^4He , and that the measured R_B is indeed anomalously low for solid helium.^{13, 14} The mag-

nitude of R_B to gaseous helium is also the same as for the liquid and solid,⁸ but of course this measurement involves a thin layer of helium on the interface. The implication is that the unknown heat-transfer mechanism is active whenever helium is present, independent of the isotope or physical state.

The reflections of phonons from interfaces with solid H_2 , D_2 , and Ne have been observed using ballistic phonon pulses.¹⁴ The results are summarized in Table I as the ratio of the measured reflection coefficient divided by that calculated using the acoustic mismatch model. The authors^{14, 15} remark that the data suggest an anomalously small R_B will exist to solid H_2 and D_2 as for He, but that R_B to solid Ne will be in accord with the acoustic mismatch theory. In view of the importance of these observations and of the uncertainty in the values quoted in Table I, we have measured R_B to solid He, H_2 , D_2 , and Ne in the temperature range of the anomaly using a steady-state technique. The two types of measurements are actually complimentary since they probe phonons incident on the interface from the cell wall at essentially two different angles, namely $\approx 0^\circ$ for the pulse technique and $\approx 45^\circ$ for the steady-state technique.

In Sec. II we briefly review the theory. Section III discusses the experimental technique, while Sec. IV presents the experimental results. A discussion of these results follows in Sec. V. In brief we find good agreement between the Ne data and the acoustic mismatch model, while R_B to solid H_2 or D_2 is anomalously small.

II. ACOUSTIC MISMATCH MODEL

The calculation of the heat flux \dot{Q} across an interface^{2, 16} is similar to the calculation of the heat current along a dielectric rod. One integrates over all phonon frequencies (giving a T^3 dependence) and over all directions of phonon propa-

TABLE I. Ratio of a measured phonon reflection coefficient to the calculated reflection coefficient between Si and several samples, as taken from Ref. 14 for phonons having a characteristic temperature of 6–7 K. A ratio of 1.0 would signify agreement with the acoustic mismatch theory. Except as indicated, the uncertainty is about ± 0.05 .

Sample	Longitudinal phonons	Transverse phonons
Liquid ^4He	0.84	0.65
Solid ^4He	0.87	0.69
Solid H_2	0.84	0.70
Solid D_2	0.84	0.75
Solid Ne	0.78 (± 0.10)	0.90 (± 0.20)

gation, then sums over the two transverse and one longitudinal modes. But, instead of the phonon mean free path, one inserts the transmission probability $w(\theta)$ for a phonon incident on the interface at angle θ . The result is $\dot{Q}/A = (4B)^{-1}(T_2^4 - T_1^4) = B^{-1}\bar{T}^3\Delta T = R_B^{-1}\Delta T$ if $\Delta T \ll \bar{T}$, where T_2 and T_1 are the temperatures on the two sides of the interface, A is its area, and B is an explicit function of the densities and phonon velocities in the two media.

The most frequently voiced criticism of this model is the problem of determining T_1 and T_2 or, equivalently, of knowing the spectra of phonons incident on the interface. The problem may be visualized by assuming a dielectric crystalline rod bisected by an imaginary plane perpendicular to its axis. The above model, naively applied, would predict a boundary resistance across the imaginary interface.² A similar difficulty arises in thermal conductivity calculations when the phonon mean free path is much longer than the sample dimensions. For the case of R_B this problem is avoided theoretically by assuming the presence of an appropriate spatial decay of the phonon distribution on both sides of the interface.^{17,18} Experimentally we avoid this problem by using metals of large thermal conductivity. Then the phonons incident on the interface from one side are produced by and are characteristic of the large, nearly isothermal sea of conduction electrons on that side of the boundary.

The electrons, however, play one additional role which must be taken into account. As in the analogous case in optics, phonons incident from the liquified or solidified gas have a critical angle beyond which there is normally total reflection from the interface. The process of reflection produces a disturbance in the second material which does not propagate away from the boundary. If a mechanism is present which absorbs or scatters phonons in the second material, a net heat transport across the interface will occur. Since electrons absorb phonons, this process will

occur for He, H_2 , D_2 , or Ne in contact with copper. Khalatnikov was aware of this process in his original theory.¹ However, he included only those phonons incident just beyond the critical angle and assumed that the appropriate absorption coefficient was essentially infinite. We, on the other hand, include all incident phonons in the modified acoustic mismatch model¹⁶ and use for the absorption coefficient the measured electron-phonon interaction constant for copper.¹⁹ The result is shown in Fig. 1 which gives the variation of $R_B T^3$ between the several liquified or solidified gases and copper as a function of phonon attenuation l^{-1} . The value of l^{-1} caused by the conduction electrons is indicated by the arrow. Other parameters used in the calculations are summarized in Table II.

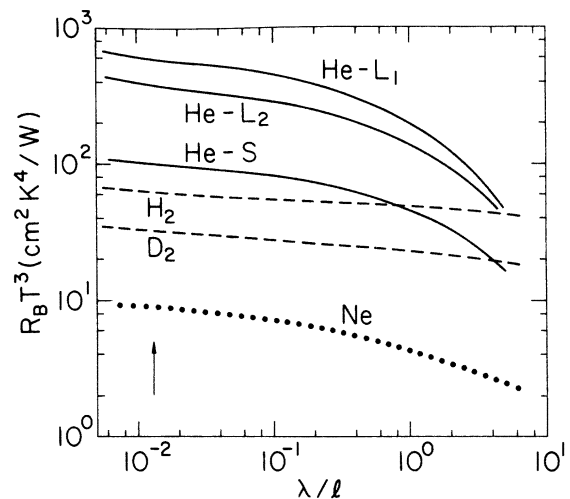


FIG. 1. Thermal boundary resistance R_B at a copper surface, multiplied by the cube of the temperature T , as a function of the phonon mean free path l and phonon wavelength λ in the copper. He- L_1 , He- L_2 , and He- S refer to liquid ^4He at 2 atm pressure, liquid ^4He at 22 atm pressure, and solid ^4He at 37 atm pressure. The arrow indicates the value of λ/l contributed by the conduction electrons of the copper.

TABLE II. Values of densities ρ and phonon velocities c used in calculating the thermal boundary resistances plotted in Fig. 1. Over the pressure range covered by the experiment there is little change in these values for the solidified gases. Thus a single calculated R_B is sufficient for comparison of theory and experiment.

Material	ρ (g/cm ³)	c_l (cm/sec)	c_t (cm/sec)
Cu	8.96	4.83×10^5 ^a	2.39×10^5 ^a
⁴ He (0 atm) ^b	0.145	2.38×10^4	
⁴ He (22 atm) ^b	0.170	3.43×10^4	
⁴ He (37 atm) ^c	0.200	5.3×10^4	2.5×10^4
H ₂ ^d	0.0882	1.95×10^5	1.15×10^5
D ₂ ^d	0.200	1.78×10^5	1.0×10^5
Ne ^e	1.507	1.13×10^5	6.33×10^4

^a O. L. Anderson, in *Physical Acoustics*, edited by W. P. Mason (Academic, New York, 1965), Vol. III B, p. 43.

^b J. Wilks, *Properties of Liquid and Solid Helium* (Oxford U.P., London, 1967).

^c D. S. Greywall, *Phys. Rev. A* **3**, 2106 (1971).

^d R. Wanner and H. Meyer, *J. Low Temp. Phys.* **11**, 715 (1973).

^e R. Balzer, D. S. Kupperman, and R. O. Simmons, *Phys. Rev. B* **4**, 3636 (1971).

III. EXPERIMENTAL TECHNIQUE

The boundary resistance measurements were made in the parallel-plate cell shown in Fig. 2. Thus the samples were sandwiched between two plates of high-purity copper. The faces of the copper plates were mechanically polished optically flat and then vacuum annealed. Small Mylar spacers kept the plates separated while the outer wall of fiber glass reinforced epoxy²⁰ was added.

A calibrated germanium resistance thermometer was screwed into each plate. Each thermometer was permanently inserted within a cylindrical copper holder; the manganin leads were thermally grounded to this cylinder, to the top plate of the cell, and to the He bath. The electrical heaters were enclosed within copper-foil boxes to contain any infrared radiation from hot heater wires. The superconducting leads from the lower heater were thermally grounded to the He bath.

Two access ports were provided through the lower plate to the sample space as shown in Fig. 2. The 0.025-cm-i.d. copper-nickel fill line went to one port and the other was sealed off after it was determined that the fill line was continuous. The fill line was thermally isolated from the He bath except by one copper link near the top of the cell. An electrical heater was wrapped around the fill line and bonded to it with GE7031 varnish. An epoxy joint was placed in the fill line near the cell so that the lower copper plate of the cell would be

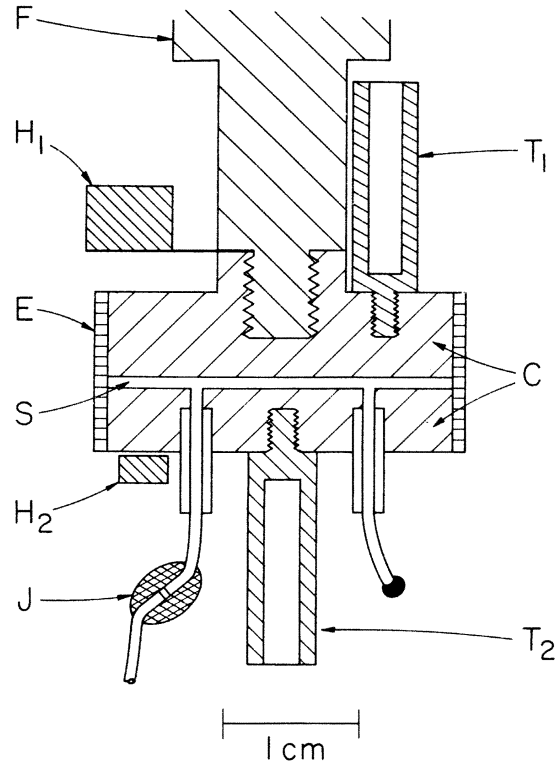


FIG. 2. Thermal boundary resistance cell. C, annealed copper plates; S, sample space; E, epoxy-fiberglass wall; J, fill line with electrical isolation; T, copper mounts for calibrated germanium resistance thermometers; H, electrical heaters; F, portion of copper flange. Heater H₂ actually extended across the bottom of the cell.

electrically isolated. This permitted capacitance measurements to be made on the cell as described below.

The cell was screwed to a copper flange which in turn was in direct contact with a He bath. This threaded joint was soldered with Ga to provide good electronic thermal contact. The bath could be pumped below 1 K and provided the relatively large refrigeration needed for the measurements.

In making a measurement the top plate of the cell was regulated at temperature T_1 using the heater H_1 . The temperature of the bottom plate was checked to be certain it also read T_1 (i.e., no spurious heat leaks were present). Heat \dot{Q} was then applied to H_2 and the temperature T_2 of the bottom plate read. The total thermal impedance Z across the cell was calculated from $ZT^3 = A(T_2^3 - T_1^3)/4\dot{Q}$. The quantity (ZT^3) was calculated in this way to remove most of the expected temperature dependence and to avoid defining and calculating ΔT and \bar{T} (see Sec. II).

The thermal impedance of the empty cell was measured, which gave $ZT^3 \approx 1.2 \times 10^4 T$ in units of

$\text{cm}^2 \text{K}^4/\text{W}$ between 1 and 2 K. This shunting impedance caused less than 2% error in the measurements involving liquid He I, and a negligible error for all other measurements.

The cell was filled at pressures up to 60 atm by passing the gas directly from a storage cylinder through a liquid-nitrogen cooled molecular-sieve trap to the cell. The starting purities were 99.9995% for H_2 and He, 99.995% for Ne, and 99.5% for D_2 . The neon was of nominal isotopic composition. The cell was flushed with the sample gas and pumped to a vacuum several times at room temperature before the final filling. The cell was then pressurized and the bath (and cell) cooled slowly until the fill line froze, after which the fill-line heater was turned off and cooling proceeded at constant sample volume. The pressure in the cell could be monitored by measuring the capacitance between the two copper plates of the cell. This was done with a guarded capacitance bridge; the capacitance versus pressure calibration was carried out with liquid He in the cell.

The total thermal impedance across the cell may be represented by the resistive circuit shown as an inset in Fig. 3. Here R_w is the thermal resistance of the wall which was discussed above. R_B is the boundary resistance, R_c is the bulk

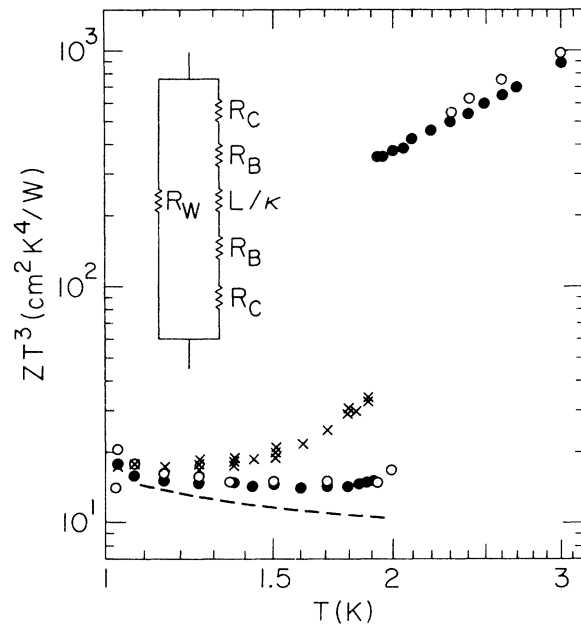


FIG. 3. Thermal impedance Z of the cell, multiplied by T^3 , vs temperature T . \circ , liquid ^4He at 2 atm; \bullet , liquid ^4He at 22 atm; \times , solid ^4He at 37 atm. The dashed line represents ZT^3 for liquid ^4He after correcting for the temperature drop within the copper plates. The insert shows the several contributions to the thermal impedance Z of the cell as discussed in the text.

thermal resistance of the copper plates, and L/κ is the bulk thermal resistance of the sample. The influence of R_c and L/κ will be discussed in Sec. IV. In the ratio L/κ , κ is the thermal conductivity of the sample and L is the separation between the two plates of the cell. A capacitance measurement gave $L = (5.8 \pm 0.6) \times 10^{-3}$ cm, the uncertainty being related to the unknown effect of fringing fields during the measurement.

The parallel-plate arrangement of Fig. 2 produces one additional source of uncertainty. If the phonon mean free path within the sample is greater than L , then the quantity $2R_B T^3$ is modified⁷ to $R_B T^3(2 - \bar{w})$, where \bar{w} is an average transmission coefficient from the copper into the sample. This is important only for Ne, for which $\bar{w} = 0.29$.

IV. RESULTS

The data for liquid and solid ^4He are shown in Fig. 3. These samples were measured both to characterize and to test the cell. Looking first at the liquid data at pressures of 2 and 22 atm, the abrupt change in ZT^3 near 2 K is associated with the superfluid transition. Above ≈ 2 K the liquid is normal (He I), and to good accuracy $ZT^3 = LT^3/\kappa$ since R_w and R_B represent only 1% effects. The κ of He I obtained from Fig. 3 agrees within 15% with the measurements of Kerrisk and Keller,²¹ as does the pressure coefficient. For $T \lesssim 2$ K the helium is superfluid, thus, $ZT^3 = 2R_B T^3 + 2R_c T^3$. As will be discussed below, the term $2R_c T^3$ related to the copper is not negligible for this case. Correction of the liquid-He II data for $2R_c T^3$ gives the dashed line shown in Fig. 3. Thus for liquid ^4He at 2 or 22 atm in the range 1–2 K, $R_B = 17T^{-3.5}$ in units of $\text{cm}^2 \text{K}^4/\text{W}$ for our samples. This is a rather typical temperature dependence and magnitude when compared with previous measurements.²²

The data for solid ^4He in Fig. 3 show an increase in ZT^3 above that of He II. Assuming this increase is related to L/κ we deduce a value for κ of solid ^4He which is in good agreement with earlier measurements.^{23,24} In brief, the cell provides reliable, quantitative data.

Figure 4 shows the data of ZT^3 for solid H_2 , D_2 , and Ne for temperatures up to 6 K. The highest temperature data were taken primarily to obtain a value for $R_c T^3$. Since the maximum in κ for solid Ne is near 2 K, the magnitude of κ above 2 K is nearly independent of sample preparation.²⁵ Hence the quantity LT^3/κ is known. (It is appreciable in the present measurements only for $T \gtrsim 3.5$ K.) Then, assuming that $2R_B T^3$ is of order $15 \text{ cm}^2 \text{K}^4/\text{W}$ throughout the temperature range and thus of minor importance above ≈ 3 K, one can deduce

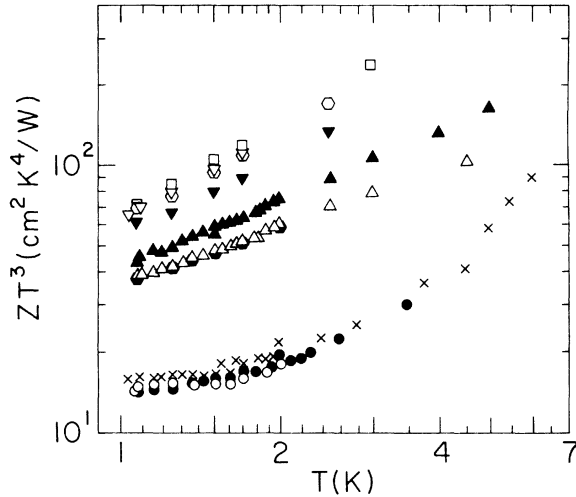


FIG. 4. Thermal impedance Z of the cell, multiplied by T^3 , vs temperature. Ne: \times , 8.5 atm; \circ and \bullet , 10 atm. D_2 : \blacktriangle , 34 atm; \triangle , 17.7 atm; closed hexagon, 4.8 atm. H_2 : \blacktriangledown , 0 atm; \square , 1 atm; ∇ , 22 atm; open hexagon, 45.6 atm.

that $2R_c T^3 = 1.2 \text{ cm}^2 \text{ K}^4/\text{W}$. This is in qualitative agreement with the value estimated for this cell design. Subtracting this quantity from the raw data of ZT^3 for $T < 2 \text{ K}$ gives the dashed line in Fig. 3 for liquid He II, and gives the corrected data for H_2 , D_2 , and Ne shown in Fig. 5.

The data for solid Ne were quite reproducible from sample to sample as may be seen in Fig. 4. This was not true for either the solid H_2 or solid D_2 . It is our opinion that the H_2 and D_2 samples were highly strained. Annealing the samples did not help, although after each anneal the samples were cooled in a highly constrained environment. Solidifying the samples at pressures ranging from ≈ 0 –46 atm did not help, nor is there a systematic shift in ZT^3 with pressure. Both the H_2 and D_2 data fit quite accurately a temperature dependence of the form $ZT^3 = a + bT$. For example, $ZT^3 = 14 + 27 T \text{ cm}^2 \text{ K}^4/\text{W}$ for D_2 at 34 atm. If we assume the second term is related to L/κ and is dominated by the scattering of phonons by the static strain fields of dislocations,²⁶ we deduce a dislocation density of $\approx 10^{11} \text{ cm}^{-2}$ which is reasonable for a highly strained material. If the remaining portion of ZT^3 were related to the boundary resistance, we would have $2R_B T^3 \approx 1$ for solid H_2 and $2R_B T^3 \approx 15$ for solid D_2 . This explanation of ZT^3 is of course pure speculation. What is more certain is that the solid H_2 and D_2 samples, in our configuration, did not behave the same as solid He and Ne.

A final remark should be added concerning solid Ne. Folinsbee²⁷ attempted to carry out a mea-

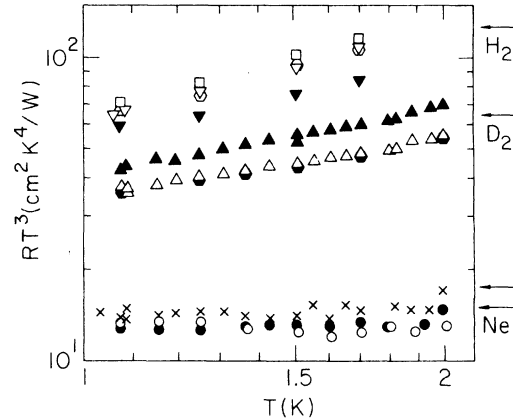


FIG. 5. Thermal impedance of cell corrected for temperature drop in the copper plates and multiplied by T^3 . The symbols are the same as in Fig. 4. The arrows on the right-hand side indicate the values of $2R_B T^3$ calculated from the acoustic mismatch theory as in Fig. 1. For Ne there is some uncertainty in this value as discussed in the text.

surement similar to the present measurements. Unfortunately the filling conditions were such that the pressure in the cell was very close to zero, and hence the cell may have been only partially filled. (From the initial conditions the cell should have been nearly full.) Thus his values of $2R_B T^3$ provided only an *upper* limit. But more importantly, $2R_B T^3$ was found to be independent of temperature from 0.4 to 1.2 K. Combining this information with that of Fig. 5, the temperature dependence of R_B for Ne from 0.4 to 2 K is found to vary quite accurately as T^{-3} . The magnitude of $2R_B T^3$ measured by Folinsbee was $17 \text{ cm}^2 \text{ K}^4/\text{W}$, or about 13% larger than the present measurements.

V. DISCUSSION

The values of $2R_B T^3$ calculated from the acoustic mismatch theory (Fig. 1) are indicated on the right-hand edge of Fig. 5. It is again emphasized that no adjustable parameters are used in the calculation, the magnitude of the phonon attenuation l^{-1} is that contributed by the conduction electrons. The ratios of the calculated values of $R_B T^3$ to the experimental values for each material are given in Table III. For solid H_2 and D_2 the smaller value is related to the ZT^3 actually measured near 1 K and is a lower limit, while the larger value is related to the $2R_B T^3$ deduced if dislocations are assumed to be present in the sample as discussed in Sec. IV and is an upper limit. For solid Ne, the range indicates the uncertainty related to the use of¹⁶ $2R_B T^3$ or $(2 - \bar{w})R_B T^3$, as discussed in Sec. III, since the phonon mean free

TABLE III. Ratio R_1 of the calculated boundary resistance divided by the measured value for a copper boundary, and the ratio r_2 (an upper limit) of the measured phonon transmission coefficient divided by the calculated value as obtained from Ref. 14 for phonons having a characteristic temperature of 6–7 K. For r_2 we have used an average value consisting of a 20% contribution from longitudinal phonons and an 80% contribution from transverse phonons. Also given is the quantum parameter η , which is roughly the ratio of the zero-point kinetic energy of the atom (molecule) divided by its potential energy.

Sample	r_1	r_2	η
Liquid ^4He ^a	83	b	0.18 ^c
Solid ^4He	13	14	0.18 ^c
Solid H_2	2–100	7.6	0.076 ^c
Solid D_2	2–4	3.7	0.035 ^d
Solid Ne	1.17 ± 0.1	1.5 ± 0.6	0.0049 ^c

^a Liquid at low pressure.

^b This should be a large but finite value since the phonons are not incident at precisely 0° .

^c L. H. Nosanow, L. J. Parish, and F. J. Pinski, Phys. Rev. B **11**, 191 (1975).

^d Calculated using Lennard-Jones parameters taken from *AIP Handbook*, 3rd Ed. (McGraw-Hill, New York, 1972), pp. 2–238.

path in the Ne is not known.

The ratios of Table III may be compared to the phonon reflection measurements of Ref. 14 if it is assumed that all phonons not detected in reflection are transmitted across the interface. The ratios of the resulting transmission coefficients, which are upper limits, divided by the calculated values, are also included in Table III. The data from the two types of experiments agree qualitatively even though the phonons used in Ref. 14 have an angle of incidence from the Si near 0° while the dominant phonons in the present work have a predominant angle of incidence from the Cu of $\approx 45^\circ$.

The phonons employed in the work of Ref. 14 had a characteristic temperature of 6–7 K. After the present paper had been submitted, additional data became available from Buechner and Maris²⁸ on the reflection coefficients between Si and solid H_2 for phonons having an estimated characteristic temperature as low as 2 K. The reflection coefficient was larger near 2 K than near 6–7 K, giving a ratio r_2 of Table III of ≈ 3.3 for the lower-temperature (lower frequency) phonons. This behavior appears not to occur for a $\text{SrF}_2 - \text{H}_2$ (or D_2) interface.¹⁵ If this behavior were present for a Cu- H_2 interface, it would be obscured in the present work by the bulk thermal resistance of the samples.

The question remains whether the unknown thermal transfer mechanism is present at the Cu-Ne

interface. The experimental data for this interface agree with the acoustic mismatch theory to $\approx 17\%$ as is typical for an interface between most “ordinary” solids.^{4,6,7} For interfaces with He, H_2 , or D_2 , on the other hand, the discrepancy is greater than 100%, which suggests that the anomaly is limited to those materials. Alternatively it may be that the anomaly is masked in the case of Ne because of the large contribution to heat transfer by the parallel acoustic mismatch mechanism. In other words $(ZT^3)_{\text{measured}}^{-1} = (2RT^3)_{\text{acoustic mismatch}}^{-1} + (2RT^3)_{\text{anomalous}}^{-1}$, from which $(2RT^3)_{\text{anomalous}} \approx 100 \text{ cm}^2 \text{ K}^4/\text{W}$. Thus the anomalous heat-transfer mechanism would have to be an order of magnitude smaller to Ne as compared to He. In brief the unknown heat-transfer mechanism is either absent or greatly diminished for an interface involving Ne. The mechanism appears to be present only in those liquids or solids most commonly referred to as quantum liquids or quantum solids. An indication of the quantum nature of the samples is given in Table III by the parameter η , which is approximately the ratio of the zero-point kinetic energy to the potential energy of the atom or molecule.

Several mechanisms have been proposed to explain the anomalously large heat transfer. As one example, it has been suggested that the acoustic mismatch theory could explain the small $R_B T^3$ if the phonon attenuation l^{-1} (Fig. 1) in the copper is sufficiently large,²⁹ perhaps in a region very close to the interface. However this effect depends primarily on the properties of the copper, not the sample.¹⁶ Since the anomalous heat transfer is present at the same copper surface for He or H_2 , but not Ne, this suggestion may be eliminated as the dominant mechanism. To be more specific, the relative effect on the several samples of increasing l^{-1} can be seen in Fig. 1 for the acoustic mismatch mechanism. Obviously the same value of λ/l cannot fit both the H_2 (D_2) and Ne data.

It has been proposed³⁰ that the atoms of the wall of atomic mass M may undergo a direct collision with the atoms (molecules) of the sample of atomic mass m such that the average transmission coefficient varies as $Mm(M+m)^{-2}$. This is not consistent with the variation of $R_B T^3$ between He, H_2 , D_2 , and Ne observed in Ref. 14 and in the present work.

It has been suggested³¹ that there may be a correlation between the transmission coefficient and ρ/c , where ρ and c are the density and average sound velocity in the sample. This contrasts with the dependence ρc found in the acoustic mismatch model. The ρ/c relationship is not compatible with the present results nor, of course, is ρc .

It might also be noted that the phonon velocity and critical angle are large for H_2 or D_2 , but small for He or Ne. Only the mass (not number) densities, as well as the quantum parameter of Table III, appear to change significantly between the anomalous materials He, H_2 , and D_2 and the normal Ne.

A number of authors³² have suggested that the anomalous heat transfer mechanism is related to some type of excitation close to or at the interface. Little can be said here in regard to this idea except that the excitation must be present for He, H_2 , or D_2 , but must be absent or nearly absent for Ne.

*Research supported in part by the National Science Foundation under Grant No. DMR-72-03026.

¹I. M. Khalatnikov, *Zh. Eksp. Teor. Fiz.* **22**, 687 (1952); *An Introduction to the Theory of Superfluidity* (Benjamin, New York, 1965), p. 138.

²W. A. Little, *Can. J. Phys.* **37**, 334 (1959).

³O. Weis, *Z. Angew. Phys.* **26**, 325 (1969).

⁴R. E. Peterson and A. C. Anderson, *Solid State Commun.* **10**, 891 (1972); H. Haug and K. Weiss, *Phys. Lett. A* **40**, 19 (1972).

⁵A brief review and bibliography is given by A. C. Anderson, in *Phonon Scattering in Solids*, edited by L. J. Challis, V. W. Rampton, and A. F. G. Wyatt (Plenum, New York, 1976), p. 1.

⁶W. Kappus and O. Weis, *J. Appl. Phys.* **44**, 1947 (1973).

⁷S. G. O'Hara and A. C. Anderson, *J. Phys. Chem. Solids* **35**, 1677 (1974).

⁸A. C. Anderson and W. L. Johnson, *J. Low Temp. Phys.* **7**, 1 (1972).

⁹R. A. Sherlock, N. G. Mills, and A. F. G. Wyatt, *J. Phys. C* **8**, 300 (1975).

¹⁰E. S. Sabisky and C. H. Anderson, *Solid State Commun.* **17**, 1095 (1975).

¹¹C.-J. Guo and H. J. Maris, *Phys. Rev. A* **10**, 960 (1974).

¹²W. Dietsche and H. Kinder, *J. Low Temp. Phys.* **23**, 27 (1976).

¹³J. T. Folinsbee and A. C. Anderson, *Phys. Rev. Lett.* **31**, 1580 (1973).

¹⁴J. S. Buechner and H. J. Maris, *Phys. Rev. Lett.* **34**, 316 (1975).

¹⁵See also C. H. Anderson, P. Call, and E. S. Sabisky, in *Phonon Scattering in Solids*, edited by L. J. Challis, V. W. Rampton, and A. F. G. Wyatt (Plenum, New York, 1976), p. 8.

¹⁶R. E. Peterson and A. C. Anderson, *J. Low Temp. Phys.* **11**, 639 (1973); R. E. Peterson, Ph.D. thesis (University of Illinois, 1972) (unpublished).

¹⁷G. Simons, *J. Phys. C* **7**, 4048 (1974).

¹⁸M. C. Phillips and F. W. Sheard, in *Phonon Scattering in Solids*, edited by L. J. Challis, V. W. Rampton, and A. F. G. Wyatt (Plenum, New York, 1976), p. 24; W. M. Visscher (private communication).

¹⁹A. C. Anderson and S. G. O'Hara, *J. Low Temp. Phys.* **15**, 323 (1974).

²⁰J. T. Folinsbee and A. C. Anderson, *J. Low Temp. Phys.* **17**, 409 (1974).

²¹J. F. Kerrisk and W. E. Keller, *Phys. Rev.* **177**, 341 (1969).

²²N. S. Snyder, *J. Low Temp. Phys.* **22**, 257 (1976), and papers cited therein.

²³F. J. Webb, K. R. Wilkinson, and J. Wilks, *Proc. R. Soc. A* **214**, 546 (1952).

²⁴L. P. Mezhov-Deglin, *Zh. Eksp. Teor. Fiz.* **49**, 66 (1965) [*Sov. Phys.-JETP* **22**, 47 (1966)].

²⁵J. E. Clemens, Ph.D. thesis (University of Illinois, 1975) (unpublished).

²⁶M. W. Ackerman, *Phys. Rev. B* **5**, 2751 (1972).

²⁷J. T. Folinsbee, Ph.D. thesis (University of Illinois, 1974) (unpublished). The OFHC (oxygen-free high-purity) copper surfaces were mechanically polished and electropolished but were not annealed.

²⁸J. S. Buechner and H. J. Maris, *Phys. Rev. B* **14**, 269 (1976).

²⁹J. L. Opsal and G. L. Pollack, *Phys. Rev. A* **9**, 2227 (1974).

³⁰T. J. Sluckin, *Phys. Lett. A* **53**, 390 (1975).

³¹L. J. Challis, *J. Phys. C* **7**, 481 (1974).

³²See Ref. 5 plus other papers included in the book.